Experimental and theoretical investigation into the difficulties of thallium incorporation into III-V semiconductors

R. Beneyton, G. Grenet, Ph. Regreny, M. Gendry, and G. Hollinger
LEOM, UMR-CNRS 5512, Ecole Centrale de Lyon, F-69134 Ecully Cedex, France

B. Canut
DPM, UMR-CNRS 5586, Université Lyon I, F-69621 Villeurbanne Cedex, France

C. Priester
IEMN/ISEN, UMR-CNRS 8520, Boîte Postale 60069, F-59652 Villeneuve d'Asq Cedex, France
(Received 10 February 2005; revised manuscript received 29 July 2005; published 27 September 2005)

The aim of this paper is to show—from both an experimental and a theoretical point of view—why it is so difficult to incorporate thallium into III-V semiconductors. The experimental part describes how $Ga_{1-x}Tl_xAs$ epilayers on GaAs(001) and $In_{1-x}Tl_xAs$ epilayers on InAs(001) can be obtained using molecular beam epitaxy (MBE). Tl is found to be much easier to incorporate into GaAs (7% over 50 nm) than into InAs (2.5% over 50 nm) despite the higher elastic stress in the former than in the latter. Once pseudomorphic $Ga_{1-x}Tl_xAs$ epilayers of sufficient thickness have been successfully obtained, the lattice and elastic parameters for the Tl-As bonding in $Ga_{1-x}Tl_xAs$ alloys are deduced by combining results from double-crystal x-ray diffraction and Rutherford backscattering (RBS) spectrometry . The theoretical part proposes a tentative explanation—within Keating's valence force field framework—for the difficulties met when incorporating Tl into III-V compounds. When incorporated into either a GaAs or an InAs bulk matrix, the Tl atoms keep away from each other by avoiding being first neighbors in the III-element sublattice, but the magnitude of the phenomenon is clearly much smaller in the InAs case than in the GaAs case. However, this effect alone cannot explain the difference between GaAs and InAs versus Tl incorporation. Turning next to surface effects, the paper demonstrates that the dimers on the InAs surface are better stabilized by the presence of Tl than are those on the GaAs surface. Last, a stronger tendency to form diluted ordered alloy clusters for GaAs than for InAs is demonstrated, which could be a reason for the greater difficulties encountered when incorporating Tl into InAs matrix than into GaAs.

DOI: 10.1103/PhysRevB.72.125209 PACS number(s): 81.05.Ea, 81.15.Aa, 81.15.Np

I. INTRODUCTION

Nowadays many long-wavelength optoelectronic devices are made from III-V alloy layers using crystal-growth techniques such as molecular beam epitaxy (MBE) or metal organic chemical vapor deposition. However, the requirements for matching the III-V alloy lattice parameters with those of the available substrates, viz., GaAs, InP, InAs, and InSb, are drastic and the currently available wavelengths can hardly be extended further. That is why when the infrared material family—based on III-V alloys containing Tl—was proposed by Van Schilfgaarde *et al.*[1–3] a few years ago, it appeared such a promising alternative. In their pioneering work, they claimed that, theoretically, TlAs and TlP were zinc-blende semimetals, which could be combined with other III-V compounds. Therefore, incorporating Tl into III-V alloys has rapidly emerged as a possible key way to cover the wavelength region from 1.7 to about 10 μm. Since then, several groups have tried to incorporate Tl into III-V compounds like InP,[4–7] InAs,[8,9] GaAs,[10–15] or InSb.[16–18] However, these works have clearly underlined that the initial prospect for easy Tl incorporation was a little overoptimistic. First, such III-V alloys containing Tl cannot be grown using MBE at standard growth temperatures (500–600 °C) and second, even in the low-temperature (LT) growth range (180–260 °C) where such growth is permitted, only a few percent of Tl can be incorporated. Moreover, even with a few percent of Tl incorporated, defects—mainly twins—occur in the epilayer for a far smaller thickness than could be anticipated from lattice-mismatching considerations alone.

The first part of the paper describes the growth of $Ga_{1-x}Tl_xAs$ epilayers on GaAs(001) and of $In_{1-x}Tl_xAs$ epilayers on InAs(001). It specifically emphasizes how their growth differs from the references, which are those of GaAs, InAs, and $Ga_{1-x}In_xAs$ grown at similar low temperatures.

The second part of the paper proposes a tentative explanation—within Keating's valence force field (VFF) framework—for the difficulties met when incorporating Tl into III-V compounds, focusing on the differences between GaAs and InAs as far as Tl incorporation is concerned.

II. EXPERIMENTAL RESULTS

We have learned from earlier work[19–24] that the main difficulty in achieving perfect single-crystal growth is to avoid both Tl droplets on the surface and twins in the bulk. In fact, the dilemma is this. On the one hand, incorporating Tl into a III-V matrix requires V-element overpressure which is as high as possible to avoid Tl droplets forming on the surface. On the other hand, because growth temperatures are low, it is

 ©2005 The American Physical Society

TABLE I. Growth conditions for the quoted samples, viz., growth rate v_g (μm/h), growth temperature T_g(°C), the BEP ratio $R_{V/III}$ of V elements to III elements, and the Tl (In) incorporation rate x (%) as gauged by RBS. The roman numbers refer to the areas labeled in Figs. 1 and 6 for GaTlAs or InTlAs, respectively. The critical thickness—i.e., the thickness at which the RHEED pattern began to reveal twinning—h_c(nm) and the final thickness—i.e., the thickness at which the growth had really stopped—h_f(nm) are also given.

Sample	Epilayer	Area	v_g (μm/h)	T_g (°C)	$R_{V/III}$	Ga	In	Tl	h_c (nm)	h_f (nm)	x (%)	Figure
EP1442	GaTlAs	I	0.9	190	4.25	4.5		4.2	25	50		2(a)
EP1443	GaTlAs	II	0.9	180	6.6	4.5		4.0	20	50	4	2(b)
EP1549	GaTlAs	III	0.9	265	5.9	4.5		4.0	50	50	3.6	2(c)
EP1555	GaTlAs	IV	0.9	215	4.9	4.5		4.2	180	180	4.4	4(a)
EP1556	GaTlAs	IV	0.9	215	4.9	4.5		4.2	120	120	4.4	4(a)
EP1557	GaTlAs	IV	0.9	215	4.9	4.5		4.2	60	60	4.4	4(a)
EP1508	GaTlAs	IV	0.9	215	4.8	4.5		4.2	350	350	4.4	4(a)
EP1374	GaTlAs	IV	0.9	200	4.6	4.5		9.4	110	120	7	4(b)
EP1372	GaTlAs	IV	0.9	200	4.7	4.5		6.5	160	170	6	4(b)
EP1448	GaTlAs	IV	0.9	210	5	4.5		4.3	350	350	4	4(b)
EP1579	GaTlAs	IV	0.9	220	4.8	4.5		2.2	300	300	3.1	4(b)
EP1580	GaTlAs	IV	0.9	220	4.9	4.5		1.7	300	300	2.6	4(b)
EP1584	GaInAs		0.9	220	5.4	4.5	2.1			300	5	5
EP1597	GaAs		0.9	225	6	4.5			200	200		5
EP1215	InTlAs	I	0.85	190	5.4		4	4.4	15	50		7(a)
EP1562	InTlAs	II	1.10	185	6.2		5.2	5.3	15	50	4	7(b)
EP1357	InTlAs	III	1.10	210	5.6		5.2	5	250	250	2.5	7(c), 9

very important to prevent excessive incorporation of the V element and thus to conduct the growth under V-element overpressure which is as low as possible. The key to success is thus to find the best compromise between substrate temperature and V-element overpressure for a high-quality layer to be grown.

The $Ga_{1-x}Tl_xAs$ and $In_{1-x}Tl_xAs$ alloys were grown in a Riber 2300 MBE reactor where As_2 molecules are provided by a high-capacity cracking cell and Ga, In, and Tl elements by conventional solid sources. The GaAs(001) and InAs(001) nonintentionally doped substrates were epiready substrates supplied by Wafer Technology. High growth temperatures were measured using an optical pyrometer while low growth temperatures were estimated from thermocouple measurements and/or from the power delivered to the heater filament. After thermal desorption of the native oxide (at 620 °C for GaAs or at 525 °C for InAs) under As_2 overpressure, a 300-nm-thick (GaAs or InAs) buffer layer was grown (at 570 °C for GaAs or at 480 °C for InAs) in order to smooth the surface. Then the samples were cooled to 300 °C under an As_2 flux. When the substrate temperature had fallen below 300 °C, the As_2 flux was switched off to avoid further As adsorption on the surface. Finally, $Ga_{1-x}Tl_xAs$ epilayers were grown on GaAs(001) or $In_{1-x}Tl_xAs$ epilayers on InAs(001).

Different analytical methods were combined to fully characterize the epilayer obtained thus. During growth, the growth mode was monitored by real-time reflection high-energy electron diffraction (RHEED) (using a 30 kV *e*-beam gun), which provided information on the epilayer thickness and its morphological modification. After growth, the sample surface morphology was probed by Nomarski optical microscopy (NOM). Its bulk crystalline quality was checked by recording the (004) and $(115)^{\pm}$ rocking curves via a double-crystal x-ray diffraction (DCXRD) apparatus equipped with a Cu $K\alpha$ source and a thick InP(001) single crystal as first crystal. Finally, the actual Tl concentration in the epilayers was gauged by Rutherford backscattering (RBS) spectrometry using 1.5 MeV $^4He^+$ ions from a Van de Graaf accelerator.

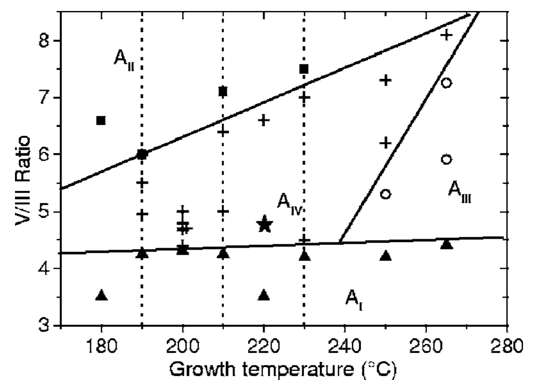

FIG. 1. Growth diagram for a 50-nm-thick $Ga_{0.96}Tl_{0.04}As$ epilayer on GaAs. (A_I) Filled triangles are for samples with metallic droplets on the surface plus twins in the bulk. (A_{II}) Filled squares are for twinned samples. (A_{III}) Open circles are for single crystals but with metallic droplets on the surface. (A_{IV}) Crosses are for single crystals with "mirrorlike" surfaces.

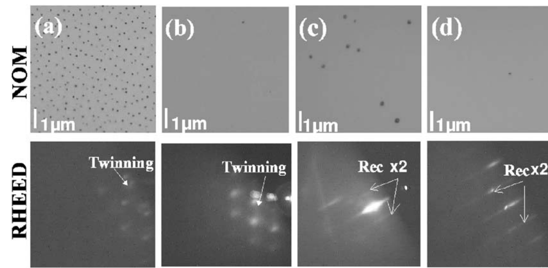

FIG. 2. Typical NOM images and RHEED diagrams along the $[\bar{1}10]$ azimuth of $Ga_{0.96}Tl_{0.04}As$ epilayers on GaAs for a sample in area (a) A_I (b) A_{II}, (c) A_{III}, and (d) A_{IV}.

In this paper, we present the growth diagrams for $Ga_{1-x}Tl_xAs$ on GaAs(001) and for $In_{1-x}Tl_xAs$ on InAs(001) as a function of the growth temperature and of $R_{V/III}$, the beam equivalent pressure (BEP) ratio of V elements to III elements. The III-element BEPs were designed to incorporate around 4% of Tl, an amount small enough to be attainable in both cases. For the sake of clarity, Table I summarizes the growth conditions concerning the samples studied in this paper. In this table, the reported III-element (Ga, In, or Tl) BEPs have not been corrected. The term "critical thickness" means the thickness at which the RHEED pattern began to reveal twinning in the epilayer while the term "final thickness" refers to the thickness at which the growth had really stopped. Finally, note that because all the atoms from the incident Tl flux are not incorporated into the layer, the nominal Tl concentration (expected from the incident III-element BEP ratio) is usually different from the Tl concentration measured by RBS. In order to provide useful reference points, GaAs on GaAs(001), InAs on InAs(001), and $Ga_{1-x}In_xAs$ on GaAs (001) were also grown under similar growth conditions.

A. $Ga_{1-x}Tl_xAs$-on-GaAs(001) growth diagram with $x\sim 0.04$

Figure 1 displays the growth diagram for $Ga_{1-x}Tl_xAs$ with $x\sim 0.04$. This composition was determined *a posteriori* by RBS. The final epilayer thickness was fixed at 50 nm. Samples in Fig. 1 have been sorted out into four different kinds depending on their RHEED patterns along the $[\bar{1}10]$ azimuth, their NOM images, and their DCXRD rocking curves. The relevant NOM images and RHEED patterns are collected in Fig. 2. Samples in area A_I [Fig. 2(a)] present a surface that is completely covered by a metallic deposit typical of a III-element-stabilized surface caused by an insufficient As supply. As a result of this metal accumulation at the surface, the RHEED pattern darkened before the epilayer reached a thickness of 20 nm. Moreover, the epilayer crystalline quality is poor as further evidenced by the presence of only one peak (attributed to the substrate) in the DCXRD rocking curve. For samples in area A_{II} [Fig. 2(b)] corresponding to higher $R_{V/III}$ and low growth temperature, the epilayers are obviously polycrystalline or even amorphous for the strongest As_2 flux. In this case, the RHEED diagram shows that a twinning process had undoubtedly begun before the epilayer was 50 nm thick. Here again, the crystalline quality of the GaTlAs epilayers is poor so that only one peak is present in the DCXRD rocking curve. When samples are grown in the third area A_{III} [Fig. 2(c)] the RHEED patterns occasionally show a weak (2×1) surface reconstruction characteristic of a smooth single-crystal growth front. NOM images demonstrate that Tl droplets are present at the surface, but unlike what is observed in area A_I, the regions between the droplets are very smooth. Therefore, one can surmise that the observed (2×1) reconstruction comes from regions free of droplets. The fourth area A_{IV} [Fig. 2(d)] is the one of interest, because it is where GaTlAs single crystals can be grown—as in area A_{III}—but without metal droplets forming on the surface. The single-crystal quality of these samples is assessed by DCXRD rocking curves showing two well-defined peaks: one for the substrate and one for the epilayer. The RHEED pattern is typical of a smooth, flat surface and very much the same as that displayed by a LT-grown GaAs layer.

Our next goal was to investigate area A_{IV} more closely. Our first step shown in Fig. 3 was to determine how long the pseudomorphic growth lasts before twinning takes place, as a function of $R_{V/III}$ [Fig. 3(a)] and as a function of Tl concentration [Fig. 3(b)]. In Fig. 3(a), the critical thickness h_c at which twinning is first detected by RHEED is determined as a function $R_{V/III}$ along the three dashed lines of Fig. 1, which corresponds to growth temperatures of 190, 210, and 230 °C. In Fig. 3(a), the dashed vertical line represents the value of $R_{V/III}$ of the frontier between areas A_I and A_{IV}, i.e., the limit between V- and III- stabilized surfaces. To the left of this vertical line, growth is typical of area A_I and the critical thickness for twinning to appear is very small. But to the right of this vertical line, i.e., in area A_{IV}, the lower $R_{V/III}$ is, the thicker the high-quality epilayer can be grown. This frontier between the A_I and A_{IV} areas appears to be a sharp singularity in the $Ga_{0.96}Tl_{0.04}As$ growth diagram. In Fig. 3(b),

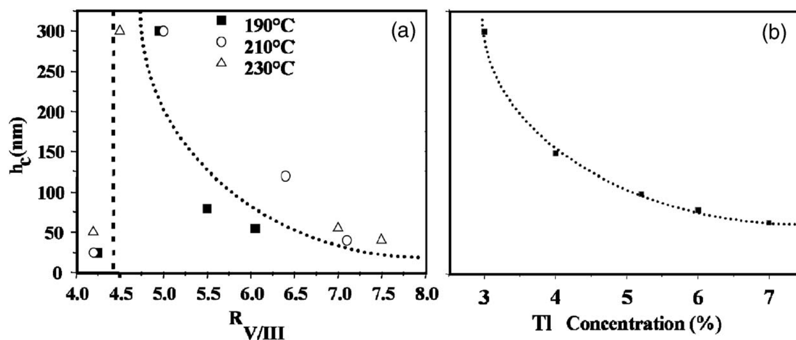

FIG. 3. Critical thickness h_c for twinning occurrence (a) as a function of $R_{V/III}$ for three growth temperatures. Filled squares for 190 °C, open circles for 210 °C, and open triangles for 230 °C. The vertical dashed line marks the frontier between area A_I (on the left) and A_{IV} (on the right). (b) as a function of Tl incorporation rate for a growth temperature of 220 °C and an $R_{V/III}$=4.8. The curved dotted line is just a guide for the eye.

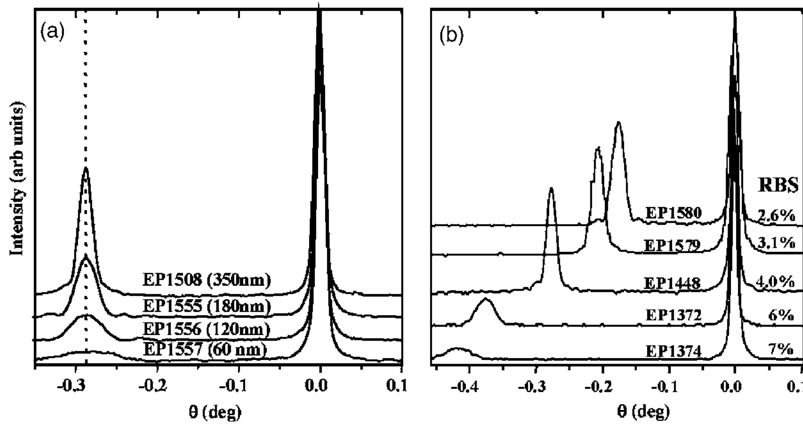

FIG. 4. DCXRD rocking curves for $Ga_{1-x}Tl_xAs$ epilayers on GaAs(001) with $x \sim 4.4$ versus (a) epilayer thickness and (b) Tl concentration. The zero corresponds to the (004) Bragg peak for the GaAs substrate.

we focused on one particular spot—indicated by a star in Fig. 1—and investigated how the twinning threshold decreased when the Tl flux increased. The twinning threshold is seen to rise faster than could be expected from lattice-mismatch considerations since it is mainly twins and not plastic dislocations that limit the attainable thickness for single-crystal growth. For example, in this temperature range, a single crystal for $Ga_{0.96}Tl_{0.04}As$ can be grown up to 300 nm but up to only 110 nm for $Ga_{0.93}Tl_{0.07}As$. The third step was to check that the growth was truly pseudomorphic until the twinning threshold is reached. In Fig. 4, we report the (004) DCXRD rocking curves of epilayers while increasing the epilayer thickness [Fig. 4(a)] or increasing Tl BEP with identical Ga BEP [Fig. 4(b)]. In Fig. 4(a) where the epilayer thickness increases from 60 nm to 120, 180, and 350 nm at a given Tl incorporation rate of 4.4%, neither the (004) DCXRD peak position nor the full width at half maximum changes, clearly indicating that there is no plastic relaxation and thus that the growth is truly pseudomorphic below the twinning threshold. In Fig. 4(b), the amount of Tl actually incorporated into the epilayer was evaluated using RBS: it ranged from 2.6% to 7%. One can see that the epilayer peak shifts toward lower and lower angles as the Tl incorporation in the GaAs matrix increases in total agreement with theoretical predictions for pseudomorphic layers.

B. Tl-As chemical bond length and elastic parameters

At this point, it was worth attempting to determine the length of the TlAs chemical bond and its elastic constants. Two main assumptions underpin this experimental determination: (i) the epilayer is strictly pseudomorphic, a point that had previously been experimentally checked, and (ii) the alloy parameter is simply given by the weighted mean of the relevant binary compound parameter, that is to say, the lattice parameter for the alloy $Ga_{1-x}Tl_xAs$ is given by $a^{\text{alloy}} = xa^{\text{TlAs}} + (1-x)a^{\text{GaAs}}$ while the elastic parameters are given by $C_{ij}^{\text{alloy}} = xC_{ij}^{\text{TlAs}} + (1-x)C_{ij}^{\text{GaAs}}$. By comparing RBS results with DCXRD, the accuracy of the TlAs binary lattice parameter and elastic constants theoretically given by Van Schilfgaarde *et al.* in Refs. 1–3 can be experimentally checked. In Fig. 5, the (004), $(115)^-$, and $(115)^+$ DCXRD rocking curves for $Ga_{0.96}Tl_{0.04}As$ on GaAs(001), $Ga_{0.95}In_{0.05}As$ on GaAs(001), and GaAs on GaAs(001) are reported. The notations $(115)^+$ and $(115)^-$ are for (115) rocking curves with high $(\theta+\alpha)$ and low $(\theta-\alpha)$ incidence angles, respectively, where θ is the Bragg peak angle and α the angle between the surface plane and the (*hkl*) plane. In our case, λ equals 0.154 051 nm, and α equals 0° for the (004) Bragg peak and 15.793° for the $(115)^{\pm}$ Bragg peak. The curve for GaAs on GaAs(001) proves that there is no As interstitial incorporation. If an excess of As were present, the DCXRD peak corresponding to the GaAs epilayer would appear to have shifted to negative angles with respect to the GaAs substrate peak. Furthermore, comparing the curves for $Ga_{0.96}Tl_{0.04}As$ on GaAs(001) and $Ga_{0.95}In_{0.05}As$ on GaAs(001) confirms that the crystal growth is of the same quality in both cases as long as the growth remains truly pseudomorphic. Experimental and calculated angular shifts are compared in Table

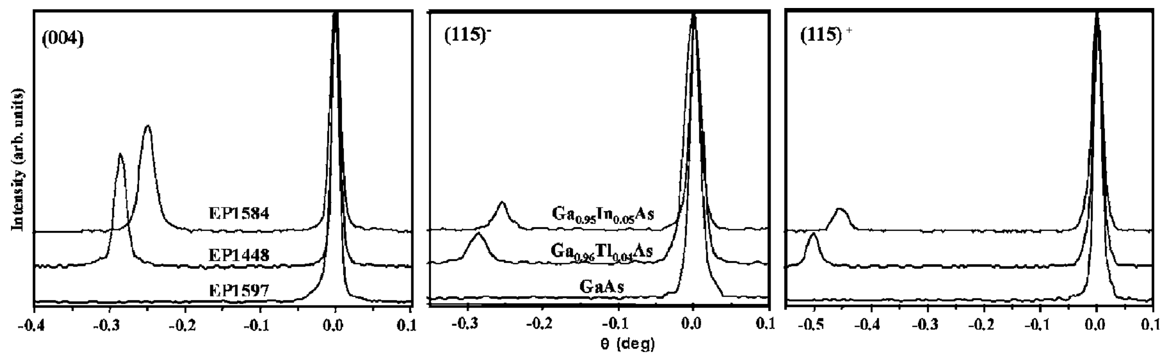

FIG. 5. Comparison of the (004), $(115)^-$, and $(115)^+$ DCXRD rocking curves for $Ga_{0.96}Tl_{0.04}As$ on GaAs(001), $Ga_{0.95}In_{0.05}As$ on GaAs(001), and GaAs(001).

TABLE II. DCXRD results for the $Ga_{1-x}Tl_xAs$ epilayers on GaAs(001) in Figs. 4 and 5.

Sample		(004) (deg)	$(115)^+$ (deg)	$(115)^+$ (deg)	DCXRD x (%)	RBS x (%)	Figure
EP1508	Expt.	−0.2880	−0.5235	−0.2948	4.4	4.4	4(a)
	Calc.	−0.2900	−0.5237	−0.2924			
EP1580	Expt.	−0.1730	−0.3180	−0.1808	2.7	2.6	4(b)
	Calc.	−0.1750	−0.3193	−0.1785			
EP1579	Expt.	−0.2100	−0.3870	−0.2153	3.2	3.1	4(b)
	Calc.	−0.2106	−0.3852	−0.2152			
EP1448	Expt.	−0.2700	−0.5063	−0.2828	4.2	4.0	4(b), 5
	Calc.	−0.2766	−0.5058	−0.2824			
EP1372	Expt.	−0.3700			5.6	~6	4(b)
	Calc.	−0.3700					
EP1374	Expt.	−0.4200			6.3	~7	4(b)
	Calc.	−0.4196					

II. Although the binary TlAs does not exist on its own, the experimental angular shifts for $Ga_{1-x}Tl_xAs$ in the range $[x=0, x=0.06]$ are in good agreement with angular shifts calculated with the parameters collected in Table III. However, for the highest Tl concentration, the epilayer starts relaxing so that the DCXRD leads to a slightly smaller Tl incorporation than RBS does. The constants for the TlAs chemical bonding, $a^{\mathrm{TlAs}}=0.618$ nm, $C_{11}^{\mathrm{TlAs}}=6.57\times10^{10}$ J/m^3, and $C_{12}^{\mathrm{TlAs}}=4.07\times10^{10}$ J/m^3, are very close to those predicted by Schilfgaarde *et al.* in their pioneering work.[1–3] They will be the input data for the theoretical part below.

Lattice mismatching cannot be the reason for the difficulties met when growing $Ga_{1-x}Tl_xAs$. As a matter of fact, if we take into account that the mismatch between GaAs and TlAs is $\epsilon=0.0853$ against $\epsilon=0.0656$ between GaAs and InAs, an epilayer of $Ga_{0.93}In_{0.07}As$ is stressed as much as $Ga_{0.95}Tl_{0.05}As$. Nonetheless, $Ga_{0.93}In_{0.07}As$ can be grown for more than 210 nm before the dislocation threshold appears, compared to only 110 nm for $Ga_{0.95}Tl_{0.05}As$. In the latter case, it is not dislocations but twins that limit the reachable epilayer thickness. We will see in the next section that despite the even lower lattice mismatch between InAs and TlAs ($\epsilon=0.0197$) the growth of $In_{1-x}Tl_xAs$ on InAs(001) is considerably more difficult than that of $Ga_{1-x}Tl_xAs$ on GaAs(001).

C. $In_{1-x}Tl_xAs$-on-InAs(001) growth diagram

A similar study was performed using InAs(001) as the substrate in order to grow $In_{1-x}Tl_xAs$ epilayers. The resulting $In_{1-x}Tl_xAs$ phase diagram is shown in Fig. 6. The expected composition of the $In_{1-x}Tl_xAs$ alloy was again $x=0.04$ but we will see below that from the RBS point of view the situation is rather more complicated. The final epilayer thickness was fixed at 50 nm as in the GaTlAs case. The corresponding NOM images and RHEED diagrams are collected in Fig. 7. In this diagram, there are only three different areas instead of the four of Fig. 1. The first area A_I [Fig. 7(a)] is similar to the A_I of Fig. 1 but for V:III BEP ratios under 4.5 instead of 4.25. To be specific, first, NOM microscopy shows that metal deposition covers the sample surface, second, the RHEED diagram darkens and becomes spotty before the sample is 15 nm thick, and third, no epilayer peak is detected in the DCXRD rocking curves due to both roughening and twinning. The second area A_{II} [Fig. 7(b)] is characterized by temperatures above 200 °C and V:III BEP ratios above 4.5. In this area A_{II}, after a few seconds of growth, the RHEED diagram becomes typical of a twinning process but the surface is still mirrorlike without any metal droplets visible at the surface. In fact, the great arsenic flux combined with a low temperature makes Tl incorporation possible (RBS indicates around 4%), but the consequence of this enforced Tl incorporation is the initiation of the twinning process. The third area A_{III} [Fig. 7(c)] is for temperatures below 200 °C

TABLE III. Lattice parameter, elastic constants, and valence force field parameters of InAs, GaAs, and TlAs.

	a (nm)	C_{11} (10^{10} J/m^3)	C_{12} (10^{10} J/m^3)	α	β
InAs	0.6058	8.33	4.53	35.18	5.50
GaAs	0.5653	11.81	5.32	41.19	8.95
TlAs	0.6180	6.57	4.07	30.00	4.0

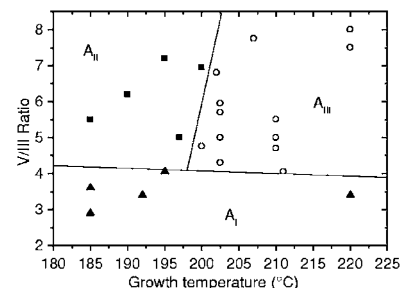

FIG. 6. Growth diagram of a 50-nm-thick InTlAs epilayer on InAs(001). (A_I) Filled triangles are for samples with metallic droplets on the surface plus twins in bulk. (A_{II}) Filled squares are for a twinned sample. (A_{III}) Open circles are for a single crystal but with Tl droplets on the surface.

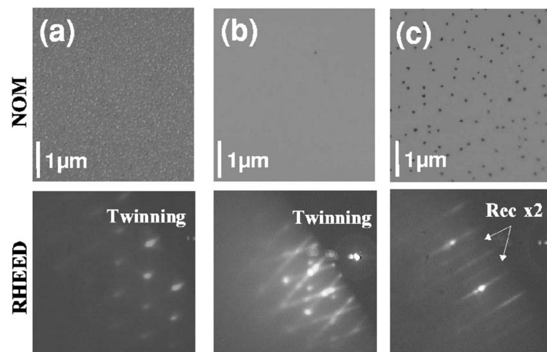

FIG. 7. Typical NOM images and RHEED diagrams along the [110] azimuth of $In_{0.975}Tl_{0.025}As$ epilayers on InAs for a sample in area (a) A_I, (b) A_{II}, and (c) A_{III}.

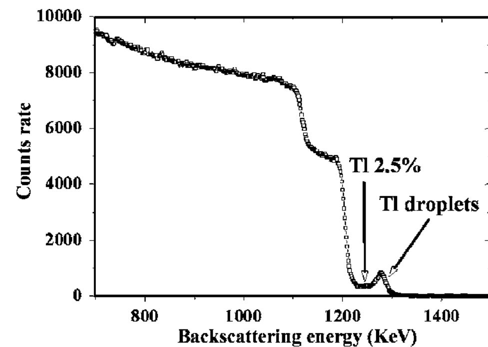

FIG. 9. RBS spectrum of InTlAs layer showing contributions from the Tl droplets on the surface and from the epilayer EP1357 with Tl concentration of 2.5%.

and V:III BEP ratios higher than 4.5. In this case, the RHEED diagram exhibits a clear (2×1) reconstruction typical of a single crystal with a smooth surface. However, when observed by NOM, the surface presents numerous metal droplets $(4.5\ 10^6/\text{cm}^2)$. Such growth front behavior is surprising because a LT InAs surface is normally only weakly reconstructed. This Tl-induced (2×1) surface reconstruction has also been seen in the $Ga_{1-x}Tl_xAs$ case but not so clearly. The greatest thickness obtained in this case before any structural defect occurred is around 250 nm. The DCXRD rocking curve for a typical sample of area A_{III} is displayed in Fig. 8. This curve (solid line) has been split into two components (dashed lines). The main peak is clearly related to the substrate but the secondary one at the lower Bragg angle can be attributed either to an actual InTlAs epilayer or to interstitial As incorporation. In this regard, the RBS spectrum shown in Fig. 9 can be of some help. It appears that the amount of Tl actually incorporated into the epilayer is hard to determine because of screening due to the Tl droplets present on the surface and responsible for the peak at 1300 keV. However, the spectrum can be simulated by two components, the first corresponding to the Tl droplets and the second to an epilayer with 2.5% of Tl. RBS shows that the amount of Tl actually in the epilayer is considerably lower than the expected 4%: the epilayer is made of an $In_{0.975}Tl_{0.025}As$ alloy rather than of an $In_{0.96}Tl_{0.04}As$ one.

To conclude this experimental part, let us make some comments on the two growth diagrams, viz., GaTlAs on GaAs(001) (Fig. 1) and InTlAs on InAs(001) (Fig. 6). Comparing them reveals that the main difference is the shrinking of area A_{IV} to almost nothing in the $In_{1-x}Tl_xAs$ case. This means that growing up to 50 nm thick is too much for an InTlAs single crystal even with a Tl concentration as low as 2.5%: either Tl atoms are expelled from the bulk as droplets, or, if they are incorporated into the bulk, they induce twins and thus crystal instability. Furthermore, especially in the InTlAs case, the Tl atoms act as a surfactant and thus are rather good at smoothing the surface by inducing a typical surface reconstruction. Plausible explanations for this unusual behavior are not straightforward at all. One can only point out the possible extension of area A_{III} (metal droplets) to the detriment of area A_{IV} in the InTlAs case. As a matter of fact, even if in both cases the III elements prefer to alloy with each other via metal bonding rather than to form III-V chemical bonding by combining separately with arsenic, the effect is probably enhanced in the InTlAs case because In and Tl are closer elements—as far as metallic properties are concerned—than Ga and Tl. Alternatively, this shrinking of area A_{IV} in the InTlAs case could be the result of an extension of area A_{II} (twinning).

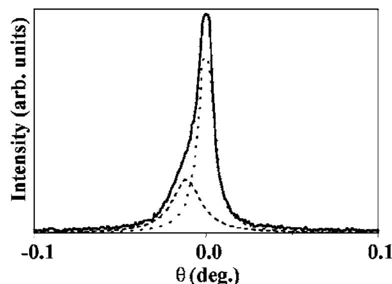

FIG. 8. DCXRD rocking curve (solid line) for InTlAs epilayers on InAs (001). The two dashed lines are for the InAs substrate and for the epilayer, respectively.

III. THEORETICAL RESULTS

In order to understand a little better why it is easier to obtain GaTlAs alloys—and with higher Tl concentration—than InTlAs, we have calculated and compared the elastic energies for different configurations involving such alloys. This study is based on an atomistic valence force field model making use of Keatings's potential.[25,26] Such a semiempirical approach has already been used to clarify some alloying effects observed during III-V MBE growth.[27,28] Its main advantage is that it allows a local atomic description not only of the bulk material but also of the surface reconstruction. This study will successively focus on three points: (i) on the interaction between Tl atoms in GaAs or InAs matrices for diluted bulk alloys, (ii) on the interconnection between (001) surface reconstruction and Tl surface concentration, and (iii) on clustering trends versus alloy dilution in a film but for atoms far enough below the surface. The three following subsections will correspond to each of the above mentioned points. Throughout this section, we will systematically compare GaTlAs on a GaAs substrate with InTlAs on an InAs substrate.

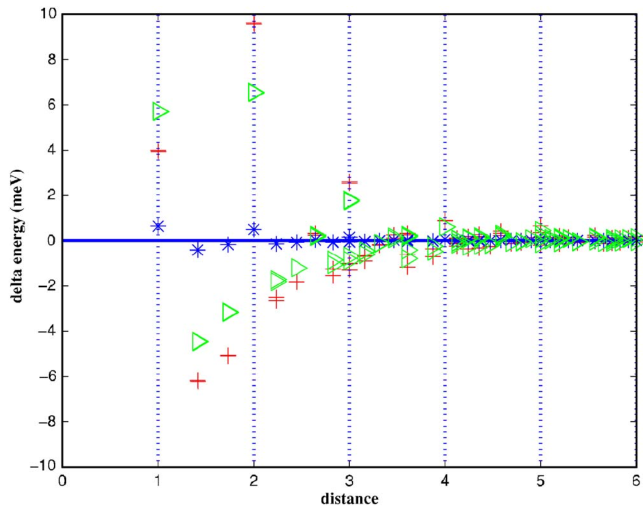

FIG. 10. (Color online) Interaction energy between two Tl atoms per period versus distance between the two Tl atoms. The interaction energy is defined as the energy for the system with two Tl per period minus twice the total energy for the system with a single Tl per period. The crosses are for GaAs:Tl, stars for InAs:Tl, and triangles for GaAs:In. The unit on the x axis is the distance between two nearest III elements, i.e., $a/\sqrt{2}$.

A. Interaction between Tl atoms in diluted bulk alloys

When a Tl atom is incorporated into a GaAs (InAs) matrix, it can be viewed as an impurity substituting for a given Ga (In) atom in the lattice. It is worth investigating in which substitution site a second Tl would better stabilize. For this purpose, we have constructed a periodical cluster made of 40 atomic planes per period in each of the three spatial directions. This three-dimensional periodic cluster is constrained in the [110] and $[\bar{1}10]$ directions (as if a binary substrate imposes its own lateral period on it) but is completely free to relax in the [001] direction (as if it were a pseudomophic alloy). The parameters used in this section are those in Table III: they are taken from the literature[26] for GaAs and InAs while for TlAs they are those given in Ref. 1 but checked by experimental evidence (see Sec. II B). The numerical scheme is as follows first, a Tl atom replaces a specified cation (Ga or In) atom. Then, a second Tl atom replaces another cation atom and the cluster is allowed to relax. The process is repeated for all possible cation sites. This way we obtain the interaction between two Tl atoms versus their relative positions. The results are reported in Fig. 10 where the reduced distance between the two Tl atoms is on axis x while the interaction energy, namely, the total energy for the system with two Tl per period minus twice the total energy for the system with a single Tl per period, is on axis y. The crosses are for GaAs:Tl, stars for InAs:Tl, and—for comparison—triangles for GaAs:In. From this study, one can clearly say that the interaction between Tl impurities is significantly stronger in GaAs than in InAs, due to the fact that the energy is mainly elastic and that the mismatch between TlAs and GaAs (9.3%) is greater than the mismatch between TlAs and InAs (2.0%). Many more details can be learned from Fig. 10. First, there are a few highly unfavorable configurations (interaction energy with positive value) and all of them correspond to a pair of atoms which are both along a [110]-type chain, an entire number of nearest cation neighbors apart (indicated by vertical dotted lines in Fig. 10). Second, there are also a few highly favorable configurations, the most attractive ones corresponding to a pair of atoms which are the nearest cation neighbors but not along a [110]-type chain. Therefore, distance is definitely not the key parameter for determining the minimum of the interaction between two Tl atoms because, depending on their location within the zinc-blende matrix, this interaction can be either attractive or repulsive (see, for example at reduced distance equal to 3). Note that this difference in mismatch—which implies a total elastic energy greater for GaTlAs than for InTlAs—cannot explain why the growth of GaTlAs is easier than that of InTlAs, but because of it, partial alloy ordering can probably be obtained more easily in GaAs than in InAs.

We can now make use of what we have just learned about this Tl interaction (five mainly undesirable relative locations within the cation centered face cubic sublattice—along the 12 [110]-like directions) to estimate the maximal Tl incorporation that respects these undesirable relative locations. For such a structure with Tl distributed within pairs of neighboring (100) planes, we obtain a critical value of 8.33% for the maximum Tl which can be incorporated into the structure. This ideal theoretical value is not so far from the measured value of 7% evoked in Sec. II A. At this stage, from bulk alloy considerations only, we do not yet have any explanation for why it is easier to grow GaTlAs than InTlAs yet, but we can say that the propensity to form partial alloy ordering is greater in GaTlAs than in InTlAs due to the greater lattice mismatching between the binaries involved. Therefore, our next step will be to go further and investigate the role of the surface in the process.

B. Reconstructed GaAs, GaTlAs, InAs, and InTlAs (001) surfaces

Usually, at standard growth temperature, As-rich (001) surfaces of III-V semiconductors are stabilized via a dimerization leading to the well-known (2×4) reconstruction. Moreover, even if the surface presents some roughness as is often the case at low growth temperature, As dimers are still present on the surface, but not necessarily aligned, leading to a (2×1) feature rather than a (2×4) reconstruction. If we consider such a (2×1) dimerized flat surface as the one schematized in Fig. 11, and if for the dimer description in Keating's potential, we use the same parameters for GaTlAs (InTlAs) as for GaAs (InAs) we can calculate and compare energies when Tl atoms are incorporated into the cation surface plane just below the dimers. As can be seen in Fig. 12, (i.e., energy per substrate atom versus Tl surface concentration) incorporating Tl into 50% of the atomic layer sites would stabilize the GaAs surface, whereas a full layer of Tl would stabilize the InAs surface. These results indicate that, during the growth of both GaTlAs and InTlAs, the surface will rapidly become Tl rich, but richer for InTlAs than for GaTlAs. This can explain why Tl droplets appear so easily on InTlAs samples. It is also worth noting that when about

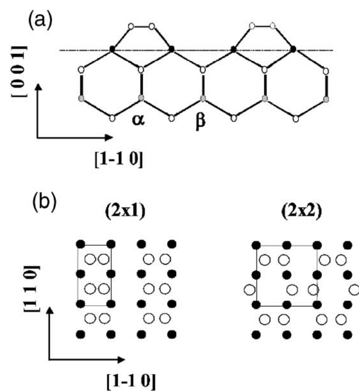

FIG. 11. Schematized views of a reconstructed surface: (a) cross section showing α and β sites; (b) plane view of a (2×1) and a (2×2) reconstructed surface.

0.75 monolayers Tl is incorporated at the GaAs surface, the more stable reconstruction for this ideally flat surface is no longer the (2×1) but a (2×2) with shifted dimers as schematized in Fig. 11(b). Note that the most stable distribution for Tl atoms corresponds to Tl distributed in lines along the dimer rows and therefore to "cation nearest neighbors."

This is clearly a surface effect which cannot be thought of any longer in terms of pairs of interacting Tl atoms (as in Sec. III A) but rather as an assembly of atoms which can collectively and softly relax because of the surface. Below this surface, one can distinguish two kinds of sites for III elements as can be seen in Fig. 11. They have been called α and β by Zunger and Co-workers.[29]. *A priori*, the β are expected to be the attractive sites for Tl atoms. Therefore, the purpose of the next subsection will be to investigate more completely first how Tl atoms will be preferentially distributed in GaTlAs and InTlAs and second how alloys can be made deeper than these first two cation surface planes.

C. Segregation strength in GaTlAs and InTlAs

To understand a little more about the difference between GaTlAs and InTlAs, we have considered several systems of alloys with a "Tl-saturated" surface and "bulk" Tl concentrations between 0.5% and 4.5%. They are either completely random bulk alloys, or more stable alloys because Tl atoms have been incorporated one by one in the energetically best cation sites. Each (001) atomic plane contains the same amount of Tl atoms. The systems are once again periodical along the $[110]$ and $[\bar{1}10]$ directions, the period being 12 atomic lines. Results can be seen in Fig. 13, where we have reported energy per substrate atom variations versus Tl bulk concentration for random GaTlAs (crosses) and InTlAs (stars) alloys, and for stabilized structures (open circles for GaTlAs and triangles for InTlAs). Note that the alloy GaInAs is very similar to GaTlAs in terms of involved-binary mismatch, and thus will follow the same general trends.

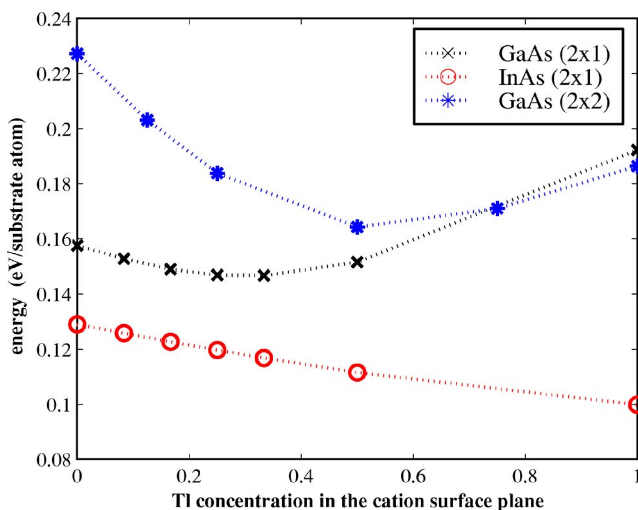

FIG. 12. (Color online) Energy variations versus Tl concentration in the cation surface layer for several GaAs and InAs reconstructed surfaces.

This figure clearly shows a stronger tendency toward lateral segregation for GaTlAs than for InTlAs: in the former case both curves are very well separated for GaTlAs, the random being the less stable one, in InTlAs alloys the two curves are hardly distinguishable. As a matter of fact, the more stable configuration—the GaTlAs case—corresponds to a clustered alloy where Tl atoms are segregated in a limited zone of a period, within two or three neighboring (100) planes but with the atoms avoiding being in nearest cation neighbor configuration (as could be predicted from Fig. 10). This can be viewed as a diluted cluster. It is interesting to note that the Tl amount in an already high-Tl-density zone does not really increase when more and more Tl is incorporated, but that the Tl atoms spread all over the period, and one can guess this will continue up to 8.33% Tl concentration. By contrast, in random alloys (more probable for InTlAs than for GaTlAs) one almost always finds two Tl atoms in nearest cation neighbor configuration. As this configuration is highly unstable, one could guess that, when this happens, another mechanism which cannot be investigated within our theoretical description, such as twin nucleation, will occur. This could explain why twins appear for lower Tl concentration in InTlAs than in GaTlAs.

We have calculated what happens for a more Tl-rich GaTlAs alloy: we observe a shoulder in the energy curve located at 8.33% Tl concentration, which corresponds to the fact that nearest cation neighbor Tl pairs can no longer be avoided (thus twins are bound to nucleate—or in the case of annealing, Tl atoms will segregate out of the alloy layer—based on what has been observed experimentally). This theoretical upper limit is slightly higher than what is experimentally observed. However, one has to keep in mind that the experiment is done at low growth temperature and therefore thermodynamical equilibrium is certainly not reached. This implies that Tl atoms would not be able to reach the best possible site and would remain as nearest cation neighbor Tl pairs, leading to a premature twinning threshold.

At this point it is interesting to note that the tendency to obtain a diluted alloy, which is mainly due to the mismatch between the two binaries, is somewhat similar in the two $Ga_{1-x}In_xAs$ and $Ga_{1-x}Tl_xAs$ cases. The actual difference between $Ga_{1-x}In_xAs$ and $Ga_{1-x}Tl_xAs$ is that in the former case, both binaries GaAs and InAs exist while in the latter case, GaAs exists but not TlAs (or it is so weakly coherent that it

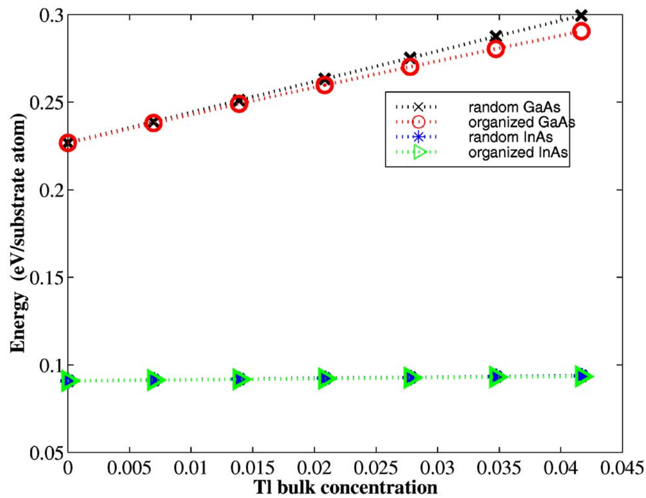

FIG. 13. (Color online) Energy variations versus Tl bulk concentration for several GaAs and InAs random or organized alloys.

cannot sustain the mixing stress). The GaAs:Tl growth is thus allowed for the GaAs matrix only insofar as Tl concentration is weak enough to prevent Tl atoms from becoming so close that they become seeds for twins. Conversely—in the $Ga_{1-x}In_xAs$ case—even if the diluted alloy expands all over the sample, incorporating more Tl is still allowed, as InAs-like areas correspond to an existing binary.

IV. CONCLUDING REMARKS

At first glance, $In_{1-x}Tl_xAs$ could seem easier to grow on InAs than $Ga_{1-x}Tl_xAs$ on GaAs because of the smaller lattice mismatch between its two binaries and thus with its given substrate. However, the experiment tells us exactly the reverse. Growing a single-crystal epilayer of $Ga_{1-x}Tl_xAs$ on GaAs(001) is much easier than growing a single-crystal epilayer of $In_{1-x}Tl_xAs$ on InAs(001) of the same thickness, containing comparable amount of Tl. In both cases, one of the main difficulties (when growing such alloys) is to prevent metal droplets forming on the surface by accurately adjusting the V: III BEP ratio. The task is more challenging for InTlAs than for GaTlAs. Drawing the growth charts has brought to light a very peculiar Tl-induced surface reconstruction which acts as an indicator for a surface's propensity to be metallized. The two phenomena are clearly concomitant: the stronger the reconstruction, the more likely it is that surface metallization will appear.

It is also clearly shown, in the case of GaTlAs for which layers of sufficient thickness and with enough Tl were successfully grown, that growth is truly pseudomorphic, but only below a critical thickness beyond which twinning occurs. The reachable epilayer thickness is thus limited not by a dislocation threshold as is classically the case, but by a twinning threshold. If too many Tl atoms replace the initial III elements, the ensuing epilayer is no longer stable under annealing: the Tl atoms migrate to the cap layer or even destroy the epilayer's integrity by segregating into structural defects.[24]

All these experimental results were compared to calculations within a VFF model, which uses Keating's potential. First of all, we demonstrated that the interaction between two Tl atoms—viewed as substitutional impurities inside the III-element sublattice—is clearly dependent on their relative locations. It is highly unfavorable to have them as pairs along the [110] direction. Even if qualitatively similar, the effect is greater for GaAs:Tl (and GaAs:In) than for InAs:Tl. At this stage, we conclude that such alloys have a natural propensity for a special organization, the magnitude of which depends mainly on the mismatch of the chemical bonding between the implicated III element and As.

We have also pinpointed both experimentally and theoretically some interaction between the ability for Tl to penetrate an InAs or GaAs matrix, and the observed surface reconstruction. Last, we have theoretically demonstrated strong segregation which forms diluted GaTlAs areas within well-defined (100) planes surrounded by pure GaAs areas. Tl atoms in such systems are spaced out enough to prevent twin nucleation (up to a critical Tl concentration estimated at about 8%). By contrast, there is no such driving force that could lead to equivalent behavior in InTlAs. That is why twins are likely to occur for lower Tl concentrations in InTlAs alloys than in GaTlAs alloys. The GaAs:Tl growth is thus possible as long as Tl concentration is weak enough to prevent Tl atoms coming so close that they act as seeds for twins. Finally, the actual difference between $Ga_{1-x}In_xAs$ and $Ga_{1-x}Tl_xAs$ is that in the former, both binaries, GaAs and InAs, exist while in the latter, GaAs exists but not TlAs.

ACKNOWLEDGMENTS

The LEOM team is grateful to F. Sanchez-Alvarez for helpful discussions and to C. Bottela and J.-B. Goure for their technical assistance on the MBE apparatus.

[1] M. van Schilfgaarde, A.-B. Chen, S. Krishnamurthy, and A. Sher, Appl. Phys. Lett. **65**, 2714 (1994).

[2] A. Sher, M. V. Schilfgaarde, S. Krishnamurthy, M. A. Berding, and A. B. Chen, J. Electron. Mater. **24**, 2714 (1995).

[3] A. B. Chen, M. V. Schilfgaarde, and A. Sher, J. Electron. Mater. **242**, 843 (1993).

[4] J. Wei, M. R. Gokhale, and S. R. Forrest, J. Cryst. Growth **203**, 302 (1999).

[5] H. Asahi, H. Koh, K. Takenaka, K. Asami, K. Oe, and S. Gonda, J. Cryst. Growth **201-202**, 1069 (1999).

[6] S. S. Chandvankar, T. K. Sharma, A. P. Shah, K. S. Chandraseran, B. M. Arora, A. K. Kapoor, D. Verma, and B. B. Sharma, J. Cryst. Growth **213**, 250 (2000).

[7] F. Sanchez-Almazan *et al.*, J. Vac. Sci. Technol. A **19**, 861

(2001).
[8] Y. Kajikawa, S. Asahina, and N. Kanayama, Jpn. J. Appl. Phys., Part 1 **40**, 28 (2001).
[9] D. I. Lubyshev, W. Z. Cai, G. L. Catchen, T. Mayer, and D. L. Miller, in *Proceeding of the 24th International Symposium on Compound Semiconductors*, San Diego, CA, 1997 (unpublished), pp. 125–130.
[10] M. D. Lange, D. F. Storm, and T. Cole, J. Electron. Mater. **27**, 5367 (1998).
[11] D. F. Storm, M. D. Lange, and L. Cole, J. Appl. Phys. **85**, 6838 (1999).
[12] H. J. Lee, A. Mizobata, K. Konishi, O. Maeda, K. Asami, and H. Asahi, J. Cryst. Growth **237-239**, 1491 (2002).
[13] Y. Kajikawa, H. Kubota, S. Asahina, and N. Kanayama, J. Cryst. Growth **237-239**, 1495 (2002).
[14] Y. Kajikawa, M. Kametani, N. Kobayashi, N. Nishimoto, Y. Yodo, Y. Kitamo, and Y. Ohtani, J. Appl. Phys. **93**, 1409 (2003).
[15] Y. Kajikawa, N. Kobayashi, and N. Nishimoto, J. Appl. Phys. **93**, 2752 (2003).
[16] C. E. C. Wood, A. Noreika, and M. Francombe, J. Appl. Phys. **59**, 3610 (1986).
[17] J. J. Lee and M. Razeghi, Appl. Phys. Lett. **76**, 297 (2000).
[18] M. J. Antonell, C. R. Abernathy, W. A. Acree, M. A. Berding, and A. Sher, J. Vac. Sci. Technol. A **17**, 338 (1999).
[19] C. T. Foxon and B. A. Joyce, J. Cryst. Growth **44**, 387 (1978).
[20] T. A. Gant, H. Shen, J. R. Flemish, L. Fotiadis, and M. Dutta, Appl. Phys. Lett. **60**, 1453 (1992).
[21] K. G. Eyink, Y. S. Cong, R. Gilbert, M. A. Capano, T. W. Haas, and B. G. Streetman, J. Vac. Sci. Technol. B **11**, 1423 (1993).
[22] M. Missou, J. Appl. Phys. **78**, 4467 (1995).
[23] M. Gandouzi, J. C. Bourgoin, L. E. Mir, M. Stellmacher, and V. Ortiz, J. Cryst. Growth **234**, 279 (2002).
[24] R. Beneyton, B. Canut, P. Regreny, M. Gendry, G. Grenet, and G. Hollinger, J. Cryst. Growth **275**, 157 (2005).
[25] P. Keating, Phys. Rev. **145**, 637 (1966).
[26] R. Martin, Phys. Rev. B **1**, 4005 (1970).
[27] X. Wallart, C. Priester, D. Deresmes, T. Gehin, and F. Mollot, Appl. Phys. Lett. **81**, 1086 (2002).
[28] X. Wallart and C. Priester, Phys. Rev. B **68**, 235314 (2003).
[29] S. Zhang and A. Zunger, Appl. Phys. Lett. **71**, 677 (1997).